ELSEVIER

ESI MS, spectroscopic and semiempirical characterization of a macrobicyclic complex with Er (III) cation

Piotr Przybylski [a], Beata Kołodziej [b], Grzegorz Leniec [c], Sławomir M. Kaczmarek [c], Eugeniusz Grech [b], Janusz Typek [c], Bogumil Brzezinski [a],*

[a] *Faculty of Chemistry, A. Mickiewicz University, Grunwaldzka 6, 60-780 Poznań, Poland*
[b] *Departament of Inorganic and Analytical Chemistry, Szczecin University of Technology, Al. Piastów 42, 70-310 Szczecin, Poland*
[c] *Institute of Physics, Szczecin University of Technology, Al. Piastów 17, 70-310 Szczecin, Poland*

Abstract

Erbium cryptate [(MSB-H+NO_3+H_2O) Er] NO_3 has been synthesized as a result of the Schiff base condensation and investigated by FT-IR, ESI MS and EPR methods. In the ESI MS spectrum of this complex [(MSB-H+NO_3+H_2O) Er] NO_3 in the range of cv = 10–30V two main signals at m/z = 422 and m/z = 842 were observed corresponding to the [(MSB-H) Er]$^{2+}$ and [(MSB-2H) Er]$^+$ fragmentary cations, respectively. Besides these main peaks, a low intensity signals at m/z = 903 and m/z = 921 assigned to the [(MSB-H+NO_3) Er]$^+$ and [(MSB-H+NO_3+H_2O) Er]$^+$ complexes were also found. FT-IR spectrum revealed a broad band at 3403 cm^{-1} assigned to the $v(OH)$ vibrations of hydrogen bonded water molecule within the 1:1 macrobicyclic Schiff base-Er^{3+} complex as well as the bands at 1335 cm^{-1} and 1355 cm^{-1} assigned to the $v(NO_3^-)$ vibrations of both bonded and non-bonded with the metal cations nitrate groups, respectively. DTA-TG analysis confirmed the presence of one water molecule in the complex. Full geometry optimization and heat of formation calculations of macrobicyclic Schiff base ligand and its complexes including nitrate anion and one water molecule were carried out. A comparison of these data suggests that the complexation of Er^{3+} cation by the macrobicyclic Schiff base molecule with the involvement of water molecule is less energetically favourable. EPR measurements confirmed the presence of one Er^{3+} cation in the complex structure. Computer simulation of the recorded EPR spectra revealed the presence of low symmetry at the Er ion site. The semiempirical MM/AM1d calculations indicated an asymmetrical location of the Er^{3+} cation within the complex structure.
© 2007 Elsevier B.V. All rights reserved.

Keywords: Macrobicyclic Schiff base; Macrobicyclic ligands; Er^{3+}; EPR; ESI MS; FT-IR; TG-DTA; Semiempirical MM/AM1d; Supramolecular chemistry

1. Introduction

Macrobicyclic ligands make an interesting group of compounds characterized by high affinity to various transition and rare earth metal cations [1–6]. Formation of supramolecular complexes between organic ligands, e.g. Schiff bases and lanthanide ions, has been often used for extraction of metal cations, on the basis of molecular recognition, catalysis of polymerization reactions, enantio-selective catalysis as well as in biomedicine applications [7–11].

The macrobicyclic ligand MSB and its various analogs (Scheme 1) have been synthesized and characterized earlier by the spectroscopic methods and X-ray analysis [12,13]. The NMR studies have clearly demonstrated that at room temperature the MSB ligand appears, irrespectively of its phase, exclusively in the imine tautomeric form and undergoes fast conformational changes in solution. From earlier studies it is well known that MSB ligand as well as its analogs readily forms complexes with various lanthanides metal cations [14–22], in which the lanthanide ion can be coordinated into the mono- or binuclear systems. Generally, the
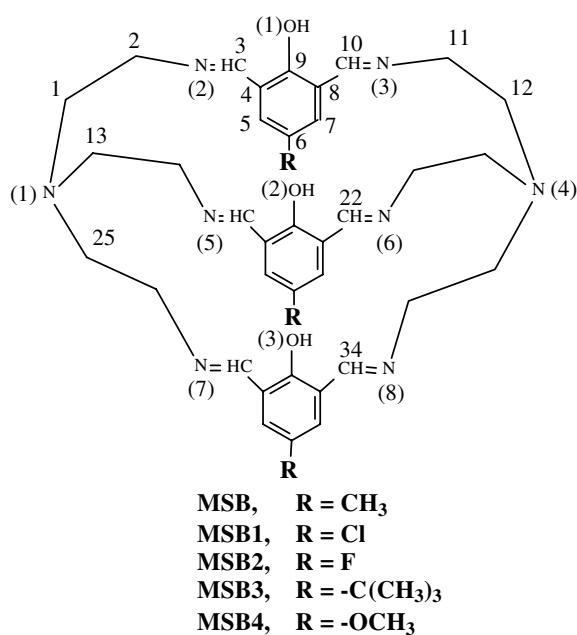
Scheme 1. The structure and the atom numbering in the MSB molecule and its various structural analogs.

complexes between MSB or its derivatives and lanthanide ions, obtained by the template synthesis, are characterized by high coordination numbers 7, 8 or 9, in which the coordination sites are substituted by counterions such as NO_3^-, ClO_4^-, SCN^- or OAc^- and H_2O or solvent molecules [12,20,21]. If the complexes of MSB or its analogs with lanthanides include the water molecule, it can be coordinated to the cation or encapsulated in the cage formed by the ligand [18,21]. The coordination geometry in the complexes of MSB and its derivatives' with lanthanides is different and depends on the coordination number, the type of complex and the kind of the counterion e.g for eight-coordinated Eu^{3+} complexes [(MSB4-3H+H_2O) Eu] and [(MSB4-2H+SCN) Eu] the coordination geometry is distorted dodecahedrons [21] while for nine-coordinated Nd^{3+} [(MSB1-2H+H_3O+NO_3) Nd]$^+$ and Dy^{3+} [(MSB+NO_3) Dy]$^{2+}$ complexes the coordination geometry is monocapped-square antiprismatic and monocapped-dodecahedron, respectively [17,19]. In some complexes formed by the MSB ligand or its analogues, a proton transfer from the phenol groups to imino nitrogen atoms was detected upon the coordination of the lanthanide or Zn^{2+}, Cd^{2+}, Pb^{2+}, Y^{3+} and Sc^{3+} metal ions [20–22].

Recently, we investigated the spectroscopic and magnetic properties of the complex of MSB and Gd^{3+} metal cation in which the monometallic substitution of the lanthanide ion into the macrobicyclic ligand cavity was detected [14]. As a continuation of these studies, in this paper we report the synthesis of erbium cryptate $C_{39}H_{47}ErN_9O_6$ as a result of Schiff base condensation and its properties determined by electrospray ionization mass spectrometry (ESI MS), Fourier transform infrared technique (FT-IR), electron paramagnetic resonance (EPR) as well as thermogravimetry and differential ther-

mal (TG-DTA) analysis. It should be mentioned that previously very similar compound was examined by Platas et al. [1] but it was chemically quite different compound: $C_{39}H_{52}ErN_{11}O_{14}$. The proposed structures of the $C_{39}H_{47}ErN_9O_6$ complexes with Er^{3+} cation were calculated and visualized by the MM/AM1d semiempirical method.

2. Experimental

2.1. Synthesis of macrobicyclic complex of MSB with Er^{3+} cation

The synthesis of the erbium complex (MSB-Er) was performed according to modified method reported previously in [12]. Tris-(2-aminoethyl)amine (tren; 1mmol) was added to solution of erbium(III) nitrate pentahydrate ($Er(NO_3)_3 \cdot 5H_2O$; 1 mmol) in hot methanol and refluxed for 10 min. Then 2-hydroxy-5-methyl-1,3-benzenedicarboxaldehyde (1.5 mmol) in methanol (100 cm^3) was added to this solution and refluxed for 30 min. A yellow solid precipitated upon cooling for 12 h. The crystalline powder was clarified by filtration. Elemental analysis for [$C_{39}H_{49}ErN_{10}O_{10}$]: Calculated: C = 47.55%, H = 5.01% N = 14.22%; Found: C = 47.53%, H = 5.00% N = 14.23%.

2.2. ESI MS spectrometry

The ESI mass spectra were recorded on a Waters/Micromass (Manchester, UK) ZQ mass spectrometer equipped with a Harvard Apparatus syringe pump. The sample solution was prepared in a mixture of acetonitrile with methanol (1:1). The measurement was performed for 1:1 complex of MSB with Er^{3+} (2×10^{-6} mol dm^{-3}). The sample was infused into the ESI source using a Harvard pump at a flow rate of 20 μl min^{-1}. The ESI source potentials were: capillary 3 kV, lens 0.5 kV, extractor 4 V. In the case of standard ESI mass spectra the cone voltage was 30 V. The spectra were also taken at different cone voltages (cv = 10, 30, 50, 70 and 90 V). The source temperature was 120°C and the dessolvation temperature was 300°C. Nitrogen was used as the nebulizing and dessolvation gas at flow-rates of 100 and 300 l h^{-1}, respectively. Mass spectra were acquired in the positive ion detection mode with unit mass resolution at a step of 1 m/z unit. The mass range for ESI experiments was from m/z = 200 to m/z = 2000.

2.3. FT-IR measurements

The Infra-Red (IR) spectra of the macrobicyclic complex of MSB with Er^{3+} cation were recorded in the mid infrared region in KBr pellets at 300 K. The spectra were taken with an IFS 113v FT-IR spectrophotometer (Bruker, Karlsruhe) equipped with a DTGS detector; resolution 2 cm^{-1}, NSS = 125. The Happ-Genzel apodization function was used.

2.4. TG-DTA analysis

TG-DTA analysis was performed using TGA/SDTA 851 of Mettler Toledo (Swiss) in the N_2 atmosphere with a heating rate of 10 K/min in the range of 300–600 K. The mass of the powder sample investigated was 8 mg.

2.5. EPR measurements

The EPR measurements were performed with a conventional X-band Bruker ELEXSYS E 500 CW-spectrometer operating at 9.5 GHz with 100 kHz magnetic field modulation. The sample, containing about 30 mg powder was placed into 4 mm diameter quartz tube. The first derivative of the power absorption spectra were recorded as a function of the magnetic field applied. Temperature dependence of the EPR spectra was recorded using an Oxford Instruments ESP helium-flow cryostat in the 3–300 K temperature range. Experimental EPR spectra were simulated by the SIMPOW computer program [23].

2.6. MM/AM1d calculations

AM1d quantum calculations were performed using the Win Mopac 2007 program at the semiempirical level (Cache Work System Pro Version 7.5 – Fujitsu)[24]. AM1d quantum semiempirical method use the Schrödinger equation to determine geometry, bond strengths, atomic hybridizations, partial charges and orbitals from the positions of the atoms and the net charge.

For the $[(MSB-H+NO_3)\ Er]^+$ and $[(MSB-H+NO_3+H_2O)\ Er]^+$ complexes, detected in the ESI MS spectra, the initial optimization of their structures was carried out using the molecular mechanics (MM) – extensive global minimum energy conformation search with the Conflex/MM3 from WinMopac 2007 program [25]. Global optimization runs were carried out for all complexes using about 2850 local minimizations in each global optimization. The calculated energetically the most favourable structures of Er^{3+} complexes, corresponding the global minimum energy points, were further optimized by the AM1d quantum semiempirical method with the energy gradient not exceeding 25 kJ mol^{-1} in one step. For all structures calculated full geometry optimization was carried out without any symmetry constraints.

2.7. Elemental analysis

The elemental analysis of the complex was carried out on Vario ELIII (Elementar, Germany).

3. Results and Discussion

The Structure of the MSB compound is shown in Scheme 1.

3.1. ESI MS studies

The ESI spectra and the main m/z signals measured at various cone voltages of the MSB-Er^{3+} complex are given in Fig. 1 and Table 1, respectively. In the ESI spectrum of this complex in the range of cv = 10–30 V two signals at m/z = 422 and m/z = 842 were observed corresponding to the mono-deprotonated and di-deprotonated 1:1 MSB-Er^{3+} complexes, respectively (cations C and B, Scheme 2). At cv = 50V these two signals were still observed and new ones of low relative intensity appeared. The intensity of these new signals could be taken as evidence of a mild fragmentation of the mono-deprotonated species proceeding with formation of di-deprotonated species. With increasing cone voltage values the signal at m/z = 842 of the di-deprotonated complex was always observed, whereas the m/z = 422 signal of the mono-deprotonated complex vanished completely and new signals appeared indicating a very complex fragmentation. The main new signals have been assigned to the cations D-G, whose structures are shown in Scheme 2. The fragmentary cations are formed by the abstraction of small neutral molecules such as H_2O, $N(CH_3)_3$ or CH_4.

Furthermore, in the extended scale of the ESI spectrum of MSB-Er^{3+} complex, recorded at cv = 30V, besides the main peaks at m/z = 422 and m/z = 842, other peak clusters at m/z = 903 and m/z = 921 assigned to the complexes $[(MSB-H+NO_3)\ Er]^+$ and $[(MSB-H+NO_3+H_2O)\ Er]^+$ are found (Fig. 2). The low intensity of the signal at m/z = 921 indicates that the water molecule is easily lost upon the complex fragmentation already at cv = 30 V. This observation demonstrates that the water molecule is rather bonded to the ligand atoms not involved in the coordination of the lanthanide ion. The calculated isotopic distributions for the peak at m/z = 905 as well as for the main peaks in the ESI MS spectrum confirm very well the proposed elementary compositions of the cations A, A1, B and C (Fig. 2).

3.2. FT-IR measurements

The FT-IR spectrum of pure MSB compound is discussed in Ref. [15]. The spectrum of the 1:1 MSB-Er^{3+} complex in the KBr pellet in Fig. 3 shows a broad band at 3403 cm^{-1} which can be assigned to the ν(OH) vibrations of a water molecule hydrogen bonded within the $[(MSB-H+NO_3+H_2O)\ Er]\ NO_3$ complex. The position of this band indicates however, that the water molecule within the complex is only weakly hydrogen-bonded, which can mean that this water molecules does not coordinate the metal cation.

Two OH phenolic groups within the complex are involved in the intramolecular hydrogen bonds with the respective nitrogen atoms of the Schiff base. Such a conclusion is confirmed by earlier CP-MAS studies [13] demon-
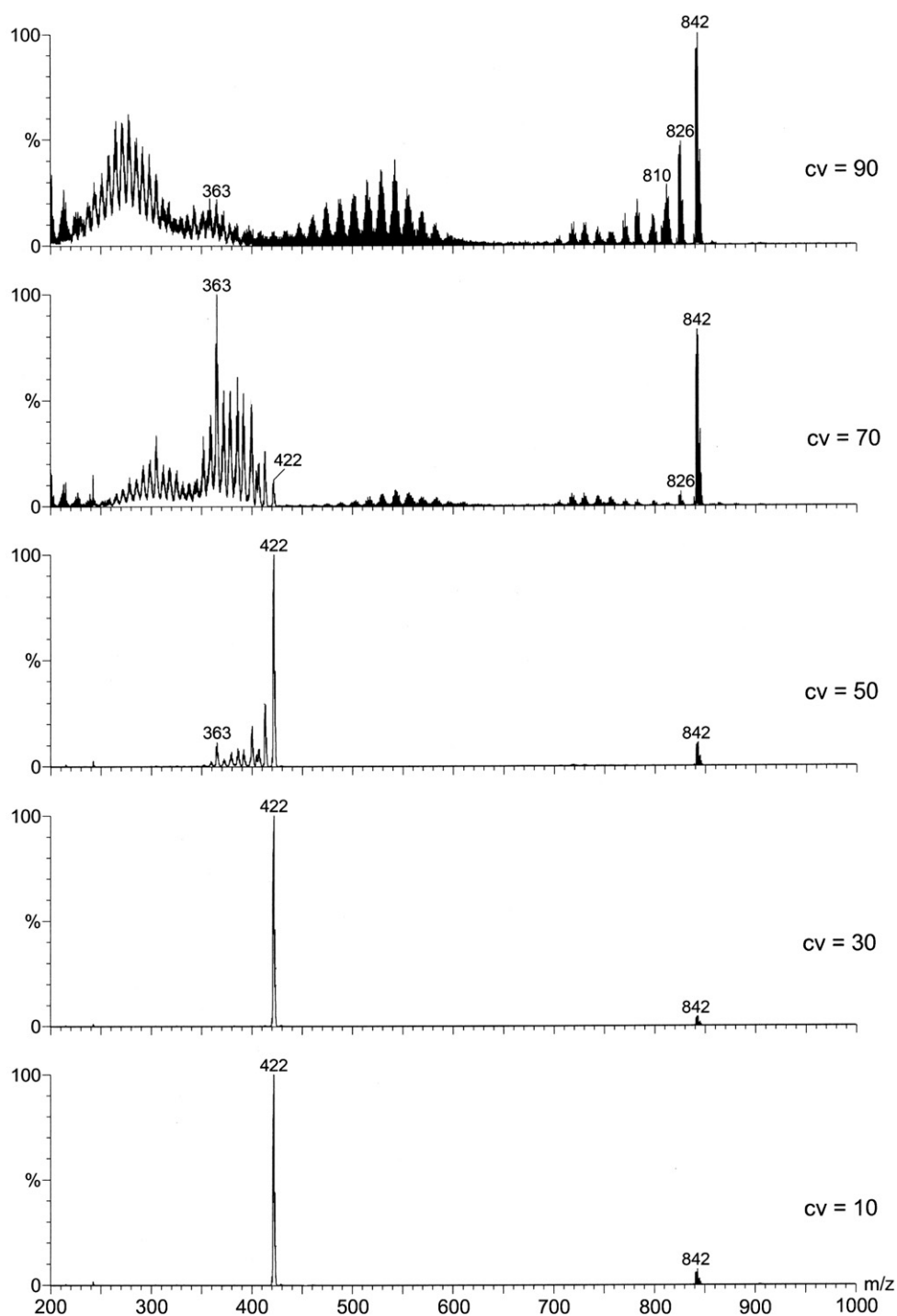
Fig. 1. The ESI MS spectra of MSB-Er^{3+} complex measured at various cone voltage values.

strating the formation of the OH···N intramolecular hydrogen bonds in which the proton is localized at the oxygen atom as well as by a broad band in the FT-IR spectrum in the region of about 3000–2000 cm^{-1}. Furthermore, the appearance of two intense bands, assigned to the $\nu(C = N)$ vibrations at 1651 and 1638 cm^{-1}, confirms the above statement. The band at 1651 cm^{-1} can be assigned to the stretching vibrations of the Schiff base groups complexed to the Er^{3+} cation and the other at 1638 cm^{-1} to the

intramolecular hydrogen bonded groups as in the pure ligand.

The presence of the NO$_3^-$ group as a ligand in the coordinating sphere is indicated by the appearance of a broadened band at ca. 1335 cm^{-1} assigned to the $\nu(NO_3)$ vibrations overlapped with the bands assigned to the $\delta_s(CH_3)$ vibrations. Furthermore, the sharp band at 1355 cm^{-1} indicates the presence of the other nitrate group non-bonded with the metal cation.

Table 1
The main peaks noted in the ESI mass spectra of the MSB-Er^{3+} complex measured at various cone voltages

Complex	Cone voltage [V]	Main peaks m/z
MSB-Er^{3+}	10	921[a], 903, 842, 422
	30	842, 422, 903
	50	842, 422, 413, 404, 363
	70	842, 826, 542, 422, 413, 404, 400, 363
	90	842, 826, 810, 542, 363, 265, 292, 278, 265

[a] The signal of a very low relative intensity.

3.3. MM/AM1d semiempirical calculations

The calculated heats of formation of pure MSB ligand (Scheme 3) and its [(MSB-H+NO$_3$+H$_2$O) Er]$^+$ and [(MSB-H+NO$_3$) Er]$^+$ complexes, all in the imine tautomeric forms, are given in Table 2. The values of the heat of formation presented in the table regarding to uncomplexed compounds, being positive one, refer to the heats calculated for a compound being yet unbounded. Comparison of these data suggests that the complexation of Er^{3+} cation by the MSB molecule without the involvement of water molecule is energetically the most favourable, whereas the structure in which one water molecule coordinates the Er^{3+} cation is less favourable than the one in which the water molecule is bonded to the ligand and does not interacts with the cation. The selected energetically favourable structures of these types of complexes are shown in Scheme 4.

The interatomic distances of the coordinating N and O atoms with Er^{3+} cation summarized in Table 3 indicate that only a part of the MSB ligand molecule (three O and four N atoms) and two oxygen atoms of the nitrate group are engaged in the coordination of the Er^{3+} cation, whereas the other part of the ligand interacts with one water molecule. Due to Er^{3+} coordination number nine, the cation achieves an almost symmetrical coordination sphere of the three-capped trigonal prism geometry (Scheme 5a). If one water molecule were involved in this coordination process of Er^{3+} cation, the symmetrical arrangement of N and O donor atoms around the cation would be strongly distorted (Scheme 5b). A comparison of the calculated interatomic distances of the coordinating N and O atoms with Er^{3+} cation with those determined for other lanthanide cations using the X-ray method demonstrates that the former coordination distances are slightly shorter. This result is understandable because the radius of the Er^{3+} cation is the smallest of the lanthanides studied earlier by X-ray methods.

3.4. TG-DTA analysis

As results from TG-DTA analysis of only a small part of the total sample mass, about 2%, is lost at about 393 K.
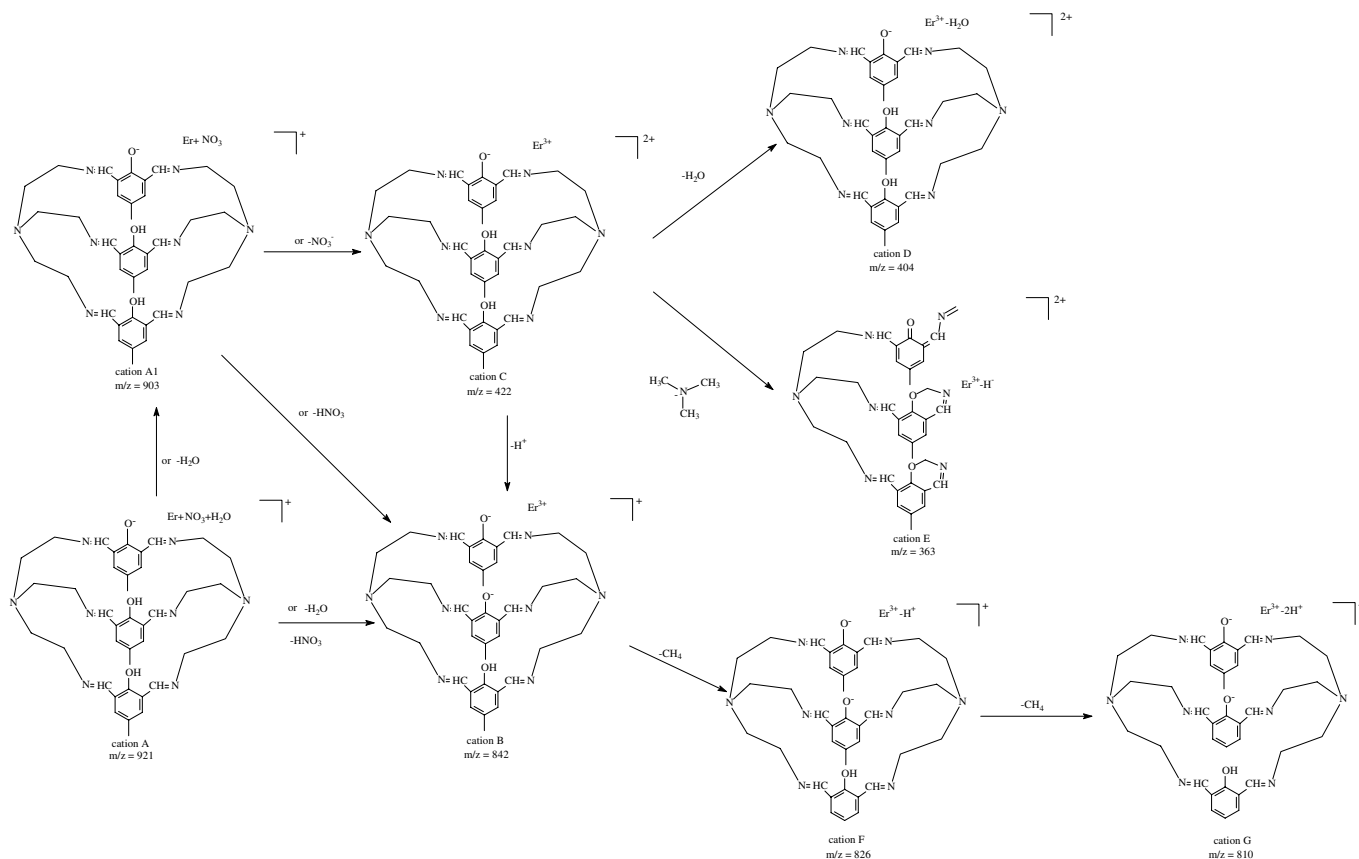
Scheme 2. The proposed direction of fragmentation of [(MSB-H+NO$_3$+H$_2$O) Er]$^+$ complex.
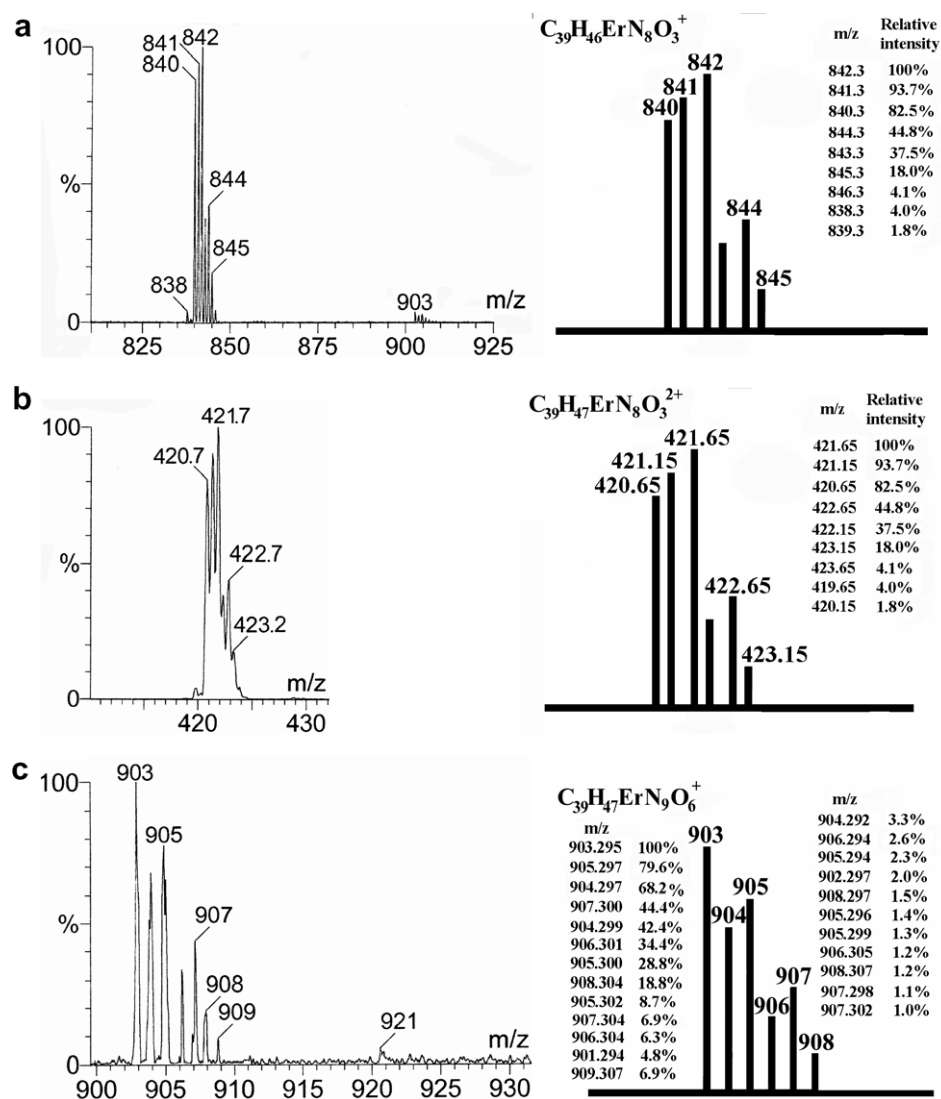
Fig. 2. The experimental (ESI MS) and the calculated isotopic distribution of the peak clusters at m/z: (a) 842 assigned to the [(MSB-2H) Er]$^+$ ion, (b) 422 assigned to the [(MSB-H) Er]$^{2+}$ complex, (c) 903 assigned to the [(MSB-H+NO$_3$) Er]$^+$ complex.

Because, on the basis of the mass spectrometry results, the total molecular weight of [(MSB-H+NO$_3$+H$_2$O) Er] NO$_3$ complex is 985 and the molecular weight of one water molecule is 18, the ratio of the molecular weight of water to the total molecular weight equals about 0.02. It is the same value as that obtained from TG-DTA analysis. It indicates that only a single H$_2$O molecule is bonded in the structure of the MSB-Er complex.

3.5. EPR studies

Fig. 4 presents the experimental EPR spectra taken at selected temperatures in the low temperature range. They reveal two main spectral components. The spectral features of these spectra are characteristic to the Er^{3+} ion with effective spin S = 1/2. The intensities of the spectral components decrease significantly with increasing temperature and above 60 K they vanish completely.

To extract the spectral parameters of the Er ion, computer simulation of the powder spectra were performed by the SIMPOW computer program. Presented in Fig. 4 simulated spectra satisfactory reproduce the experimental ones apart from the low magnetic part below 50 mT. This discrepancy may be due to not taking into account the contribution to the spectra arising from the spectral components in negative magnetic fields.

To extract the symmetry of the crystal field acting on Er ion in the complex the anisotropic g-factors were calculated using the SIMPOW computer program. In Fig. 5 the temperature dependence of the obtained g-factors is displayed. Three rather very different values of g-factors along the paramagnetic complex principal axes were obtained, as e.g. g$_x$ = 6, g$_y$ = 12 and g$_z$ = 4 calculated at 5.2 K. It indicates a low symmetry site of the Er^{3+} ion in accordance with the above presented molecular mechanics and semiempirical calculations. The thermal dependence of
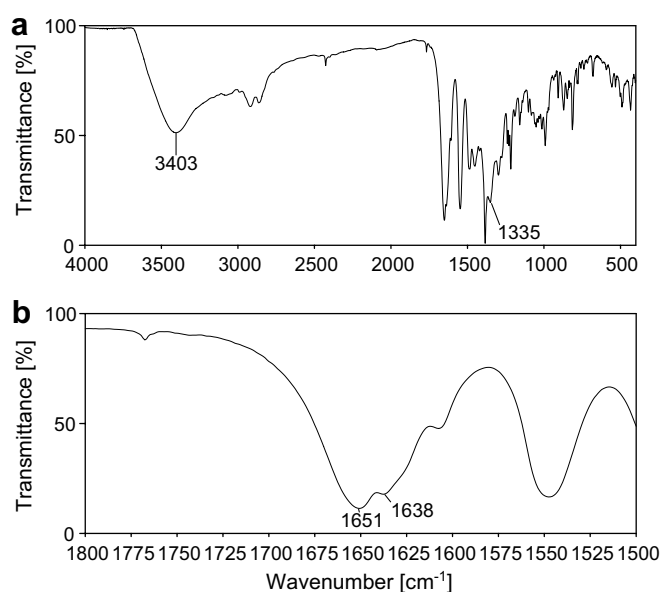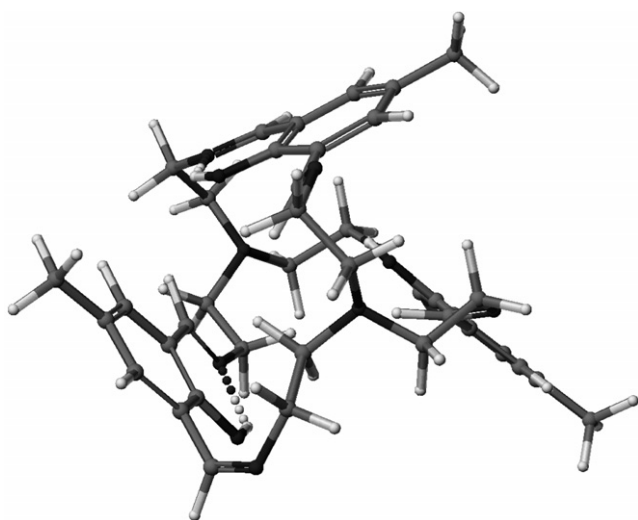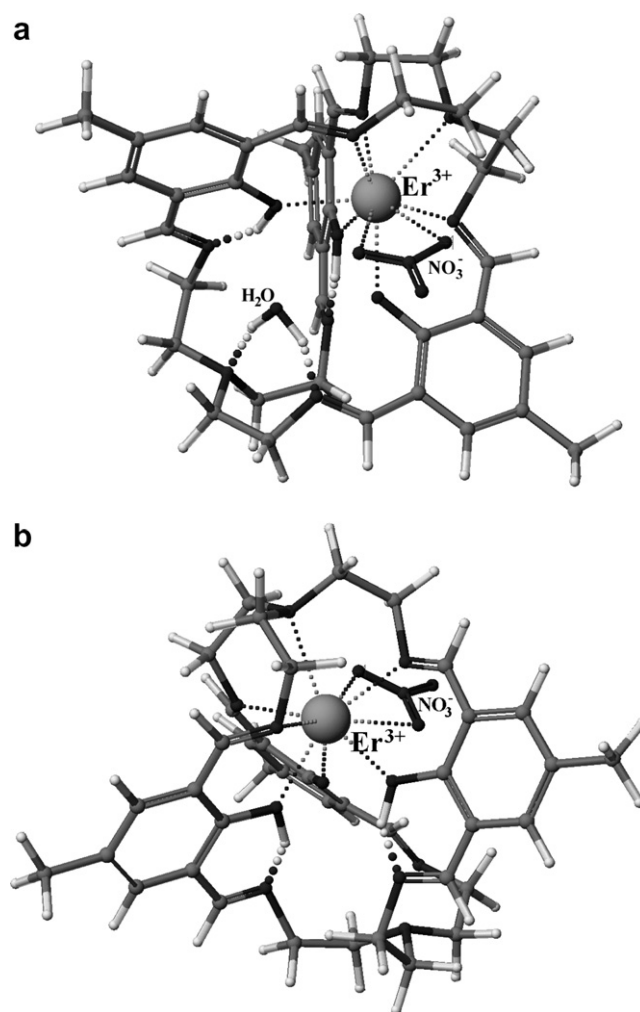
Fig. 3. The FT-IR spectrum of MSB-Er^{3+} complex in KBr pellets in the ranges: (a) 4000–400 cm^{-1} and (b) 1800–1500 cm^{-1}.

Scheme 4. The structure of: (a) [(MSB-H+NO$_3$+H$_2$Oe) Er]$^+$ (b) [(MSB-H+NO$_3$) Er]$^+$ ions, calculated by the MM/AM1d method.

g-factors evidences an increasing magnetic anisotropy of the complex with increasing temperature.

4. Conclusions

IR measurements revealed a broad band at 3403 cm^{-1} assigned to the ν(OH) vibrations of hydrogen bonded

Scheme 3. The structure of MSB calculated by the MM/AM1d method.

Table 2
Heats of formation (kJ/mol) of MSB-Er^{3+} ions, detected in the ESI MS experiment, calculated by the MM/AM1d method

m/z (ESI MS)	Cation	HOF [kJ/mol]	ΔHOF [kJ/mol]
–	MSB	−398.17	–
921	[(MSB − H + NO$_3$ + H$_2$O$_c$)Er]$^+_{uncomplexed}$	+43.84	−397.11
	[(MSB − H + NO$_3$ + H$_2$O$_c$)Er]$^+_{complexed}$	−353.27	
921	[(MSB − H + NO$_3$ + H2O$_e$)Er]$^+_{uncomplexed}$	+43.84	−475.73
	[(MSB − H + NO$_3$ + H$_2$O$_e$)Er]$^+_{complexed}$	−431.89	
903	[(MSB − H + NO$_3$)Er]$^+_{uncomplexed}$	+36.29	−593.69
	[(MSB − H + NO$_3$)Er]$^+_{complexed}$	−557.40	

ΔHOF = HOF$_{complexed}$ − HOF$_{uncomplexed}$.
H$_2$O$_c$ –water molecule very weakly coordinated to the Er^{3+} ion.
H$_2$O$_e$ –water molecule not coordinated to the Er^{3+} ion but bonded in the cage formed by the MSB ligand.

Table 3
Selected structural parameters of MSB-Er^{3+} complexes calculated by the quantum semiempirical MM/AM1d method compared to the experimental data of other complexes of **MSB** and **MSB1** with lanthanides ions (Dy^{3+}, Eu^{3+}, Nd^{3+} and Ce^{3+}) obtained by the X-ray method

|	[(MSB-H+NO3) Er]$^+$ PM5	[(MSB-H+NO3+H2Oe) Er]$^+$ PM5	[(MSB+NO3) Dy]$^{2+}$ X-ray[c]	[(MSB1+NO3+H2O) Eu]$^{2+}$ X-ray[d]	[(MSB1-2H+NO3+H3O) Nd]$^+$ X-ray[e]	[(MSB+NO3) Ce]$^{2+}$ X-ray[f]
Bond length [Å]						
M–O(1)	2.239	2.240	2.297(6)	2.288(6)	2.329(2)	2.381(5)
M–O(2)	2.315	2.362	2.344(6)	2.374(6)	2.431(2)	2.425(5)
M–O(3)	2.288	2.291	2.285(7)	2.418(6)	2.421(2)	2.424(5)
M–O(NO$_3^-$)	2.598	2.601	2.620(7)	2.649(7)	2.653(2)	2.692(5)
M–O(NO$_3^-$)	2.411	2.415	2.417(7)	2.491(7)	2.578(2)	2.641(5)
M–N(3)	2.576	2.512	2.511(7)	2.532(7)	2.585(2)	2.680(6)
M–N(4)bridge	2.691	2.690	2.695(7)	2.761(7)	2.747(2)	2.758(6)
M–N(6)	2.418	2.421	2.488(8)	2.562(7)	2.567(2)	2.649(6)
M–N(8)	2.547	2.554	2.517(8)	2.492(7)	2.543(2)	2.629(6)
M–O$_{H2O}^a$, **M**–O$_{H3O+}^b$	–	3.121^a	–	3.070(6)^a	3.023(5)^b	–
Distances [Å]						
N(1)–N(4)	8.335	8.340	8.687(7)	8.407(7)	8.381(5)	8.48(6)
C(22)–N(6)	1.267	1.268	–	1.260(11)	1.275(4)	–
C(34)–N(8)	1.288	1.289	–	1.289(12)	1.250(4)	–
C(10)–N(3)	1.274	1.275	–	1.281(12)	1.272(4)	–
Angle [°]						
O(1)–**M**–O(2)	79.11	79.64	–	78.5(2)	78.87(6)	78.04(17)
O(2)–**M**–O(3)	70.02	68.23	–	70.8(2)	69.26(6)	96.50(17)
O(2)–**M**–N(8)	73.64	74.11	–	83.8(2)	70.33(7)	70.06(17)
N(8)–**M**–N(3)	132.19	135.76	–	128.1(2)	64.66(8)	125.40(18)
O(NO$_3^-$)–**M**–N(4)	71.48	71.49	–	73.9(2)	70.32(7)	73.17(17)
O(NO$_3^-$)–**M**–O(NO$_3^-$)	47.28	47.25	–	49.7(2)	47.98(7)	47.77(16)

M = metal cation.
[c] Data from Ref. [16].
[d] Data from Ref. [17].
[e] Data from Ref. [18].
[f] Data from Ref. [14].
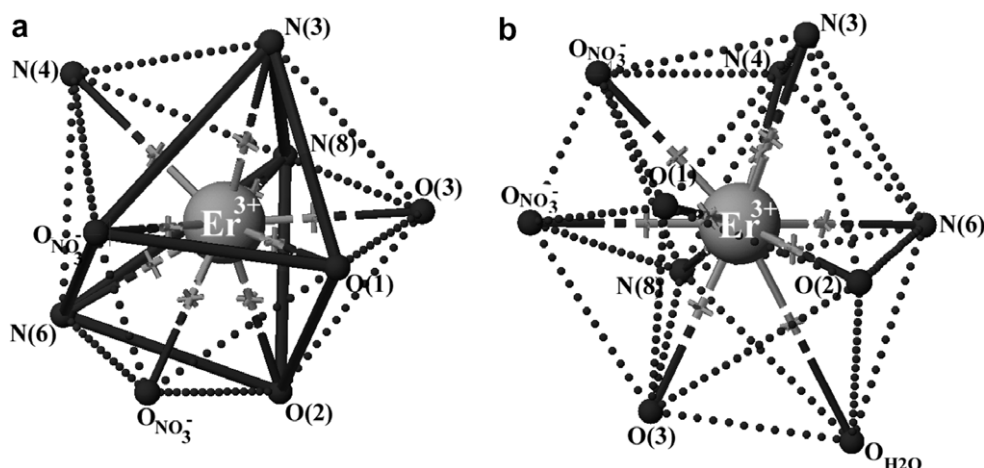
Scheme 5. A perspective view of the structure of the coordination polyhedron of the cations: (a) [(MSB-H+NO$_3$) Er]$^+$, (b) [(MSB-H+NO$_3$+H$_2$Oc) Er]$^+$, calculated by the MM/AM1d method.

water molecule within the 1:1 MSB-Er^{3+} as well as a bands at 1335 cm^{-1} and 1355 cm^{-1} assigned to the $v(NO_3^-)$ vibrations of bonded and non-bonded nitrate groups with the metal cation, respectively.

As results from TG-DTA analysis only a small part of the total sample mass of MSB-Er^{3+} complex, about 2%, is lost at about 393 K. It indicates that only a single H$_2$O

molecule is bonded in the structure of the MSB-Er complex.

Three different values of g-factors along the paramagnetic complex principal axes were obtained from SIM-POW program analysis. It indicates on a low symmetry site of the Er^{3+} ion on MSB-Er^{3+} complex in accordance with the above presented molecular mechanics and semi-
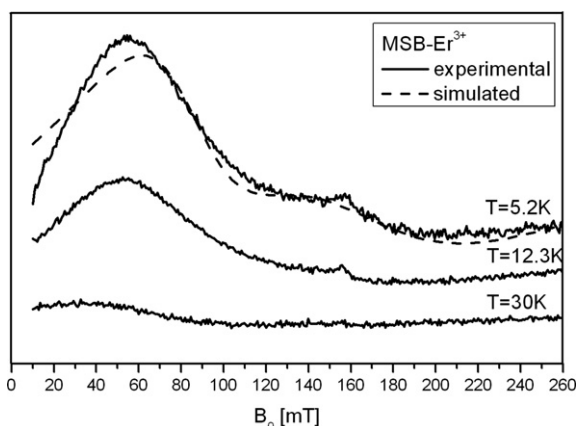
Fig. 4. EPR spectra for several temperatures in the low temperature range. Comparison of the experimental (continuous line) and calculated (dashed line) spectrum of Er ion at 5.2 K.
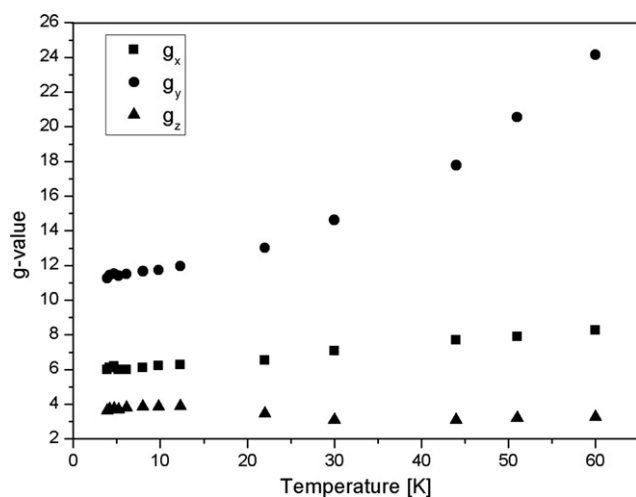

Fig. 5. Temperature dependence of the calculated anisotropic g-factors.

empirical calculations. The thermal dependence of g-factors evidences an increasing magnetic anisotropy of the complex with increasing temperature. EPR measurements confirmed the presence of one Er^{3+} cation in the complex structure.

In the ESI MS spectrum of this complex in the range of cv = 10–30 V two main signals at m/z = 422 and m/z = 842 were observed corresponding to the $[(MSB-H) Er]^{2+}$ and $[(MSB-2H) Er]^{+}$ fragmentary cations, respectively. Besides these main peaks, a low intensity signals at m/z = 903 and m/z = 921 assigned to the $[(MSB-H+NO_3) Er]^{+}$ and $[(MSB-H+NO_3+H_2O) Er]^{+}$ complexes were also found.

Full geometry optimization and heat of formation calculations of macrobicyclic Schiff base ligand and its complexes including nitrate anion and one water molecule were carried out. A comparison of these data suggests that the complexation of Er^{3+} cation by the macrobicyclic Schiff base molecule with the involvement of water

molecule is less energetically favourable in the gas phase. The semiempirical MM/AM1d calculations indicated an asymmetrical location of the Er^{3+} cation within the complex structure.

Acknowledgment

References

[1] C. Platas, F. Avecilla, A. de Blas, C.F.G.C. Geraldes, T. Rodriguez-Blas, H. Adams, J. Mahia, Inorg. Chem. 38 (1999) 3190.
[2] M. Thirumavalavan, P. Akilan, P. Amudha, M. Kandaswamy, Polyhedron 23 (2004) 519.
[3] A. Ingham, M. Rodopoulos, K. Coulter, T. Rodopoulos, S. Subramanian, A. McAuley, Coord. Chem. Rev. 233–234 (2002) 255.
[4] W.-K. Wong, H. Liang, J. Guo, W.-Y. Wong, W.-K. Lo, K.-F. Li, K.-W. Cheah, Z. Zhou, W.-T. Wong, European J. Inorg. Chem. 4 (2004) 829.
[5] J. Fan, W. Liu, N. Tang, Y. Tang, M. Tan, K. Yu, J. Rare Earths 20 (2002) 378.
[6] V.S. Sastri et al., Modern aspects of rare-earths and complexes, Elsevier B.V., Amsterdam, 2003.
[7] L. Di Bari, P. Salvadori, Coord. Chem. Rev. 249 (2005) 2854.
[8] M. Bottrill, L. Kwok, N.J. Long, Chem. Soc. Rev. 35 (2006) 557.
[9] I. Kostova, Curr. Med. Chem. - Anti-Cancer Agents 5 (2005) 591.
[10] W. Radecka-Paryzek, V. Patroniak, J. Lisowski, Coord. Chem. Rev. 249 (2005) 2156.
[11] E. Brunet, O. Juanes, J.C. Rodriguez-Ubis, Curr. Chem. Biol. 1 (2007) 11.
[12] F. Avecilla, R. Bastida, A. de Blas, D.E. Fenton, A. Macias, A. Rodriguez, T. Rodriguez-Blas, S. Garcia-Granda, R. Corzo-Suarez, J. Chem. Soc., Dalton Trans. (1997) 409.
[13] W. Schilf, B. Kamieński, B. Kołodziej, E. Grech, Z. Rozwadowski, T. Dziembowska, J. Mol. Struct. 615 (2002) 141.
[14] G. Leniec, S.M. Kaczmarek, J. Typek, B. Kołodziej, E. Grech, W. Schilf, J. Phys. Condens. Matter 18 (2006) 9871.
[15] M. Thirumavalavan, P. Akilan, M. Kandaswamy, Polyhedron 25 (2006) 2623.
[16] F. Avecilla, A. de Blas, R. Bastida, D.E. Fenton, J. Mahia, A. Macias, C. Platas, A. Rodriguez, T. Rodriguez-Blas, Chem. Commun. (1999) 125.
[17] C. Platas, F. Avecilla, A. de Blas, T. Rodriguez-Blas, C.F.G.C. Geraldes, E. Toth, A. Merbach, J.-C.G. Bunzli, J. Chem. Soc., Dalton Trans. (2000) 611.
[18] Q.-Y. Chen, C.-J. Feng, Q.-H. Luo, C.-Y. Duan, X.-S. Yu, D.-J. Liu, Eur. J. Inorg. Chem. (2001) 1063.
[19] C.-J. Feng, Q.-H. Luo, C.-Y. Duan, M.-C. Shen, Y.-J. Liu, J. Chem. Soc., Dalton Trans. (1998) 1377.
[20] M.G.B. Drew, O.W. Howarth, C.J. Harding, N. Martin, J. Nelson, J. Chem. Soc., Chem. Commun. (1995) 903.
[21] S.-Y. Yu, Q. Huang, B. Wu, W.-J. Zheng, X.-T. Wu, J. Chem. Soc., Dalton Trans. (1996) 3883.
[22] M.G.B. Drew, O.W. Howarth, G.G. Morgan, J. Nelson, J. Chem. Soc., Dalton Trans. (1994) 3149.
[23] M.J. Mombourquette, J.A. Weil, D.G. McGavin, EPR-NMR User's Manual, Department of Chemistry, University of Saskatchewan, Saskatoon, SK, Canada.
[24] CAChe WS Pro 7.5.0.85 UserGuide, Fujitsu 2007.
[25] P. Przybylski, A. Huczyński, B. Brzezinski, J. Mol. Struct. 826 (2007) 156.